

# Highly Strained Heterometallacycles of Group 4 Metallocenes with Bis(diphenylphosphino)amide Ligands

Martin Haehnel, Sven Hansen, Anke Spannenberg, Perdita Arndt, Torsten Beweries,\* and Uwe Rosenthal\*<sup>[a]</sup>

Dedicated to Prof. Heinz Berke on the occasion of his 65<sup>th</sup> birthday

**Abstract:** A study regarding coordination chemistry of the bis(diphenylphosphino)amide ligand Ph<sub>2</sub>P-N-PPh<sub>2</sub> at Group 4 metallocenes is presented herein. Coordination of *N,N*-bis(diphenylphosphino)amine (**1**) to [(Cp<sub>2</sub>TiCl)<sub>2</sub>] (Cp = η<sup>5</sup>-cyclopentadienyl) generated [Cp<sub>2</sub>Ti(Cl)P(Ph<sub>2</sub>)N(H)PPh<sub>2</sub>] (**2**). The heterometallacyclic complex [Cp<sub>2</sub>Ti(κ<sup>2</sup>-*P,P*-Ph<sub>2</sub>P-N-PPh<sub>2</sub>)] (**3Ti**) can be prepared by reaction of **2** with *n*-butyl-

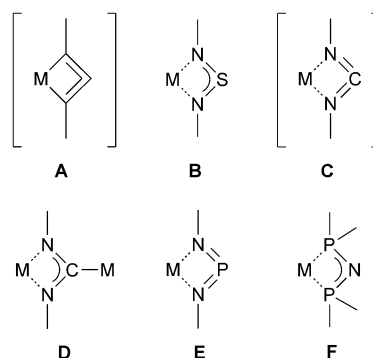
lithium as well as from the reaction of the known titanocene–alkyne complex [Cp<sub>2</sub>Ti(η<sup>2</sup>-Me<sub>3</sub>SiC<sub>2</sub>SiMe<sub>3</sub>)] with the amine **1**. Reactions of the lithium amide [(thf)<sub>3</sub>Li{N(PPh<sub>2</sub>)<sub>2</sub>}] with [Cp<sub>2</sub>MCl<sub>2</sub>] (M = Zr, Hf) yielded the

corresponding zirconocene and hafnocene complexes [Cp<sub>2</sub>M(Cl){κ<sup>2</sup>-*N,P*-N-(PPh<sub>2</sub>)<sub>2</sub>}] (**4Zr** and **4Hf**). Reduction of **4Zr** with magnesium gave the highly strained heterometallacycle [Cp<sub>2</sub>Zr(κ<sup>2</sup>-*P,P*-Ph<sub>2</sub>P-N-PPh<sub>2</sub>)] (**3Zr**). Complexes **2**, **3Ti**, **4Hf**, and **3Zr** were characterized by X-ray crystallography. The structures and bondings of all complexes were investigated by DFT calculations.

**Keywords:** density functional calculations • hafnium • metallacycles • titanium • zirconium

## Introduction

Ring-strained metallacycles of Group 4 metallocenes have been of great interest in our studies over the last decades.<sup>[1–3]</sup> In this context, the synthesis of three-membered and five-membered rings, such as metallacycloprenes, 1-metallacyclopent-3-yne, or 1-metallacyclopenta-2,3,4-trienes, could be realized. The preparation of the corresponding all-carbon four-membered metallacyclobuta-2,3-diene (Scheme 1, **A**) was not successful until now; however, a theoretical study predicted its existence and described various approaches for its synthesis.<sup>[4]</sup> Additionally, the incorporation of heteroatoms into the ring systems was found to be an elegant way for stabilizing highly strained structures.<sup>[1,4]</sup> Therefore, we focused on the synthesis of four-membered heterometallacycles of Group 4 metallocenes. Reaction of the sulfurdiiimide Me<sub>3</sub>SiN=S=NSiMe<sub>3</sub> with [Cp<sub>2</sub>M(L)(η<sup>2</sup>-Me<sub>3</sub>SiC<sub>2</sub>SiMe<sub>3</sub>)] (Cp = η<sup>5</sup>-cyclopentadienyl; M = Ti, no L; M = Zr, L = pyridine) led to the formation of four-membered metallacycles containing the metal, nitrogen, and sulfur (Scheme 1, **B**).<sup>[5]</sup> By using carbodiimides as substrates, the reactivity becomes more diverse and depends on both the



Scheme 1. Different four-membered metallacycles.

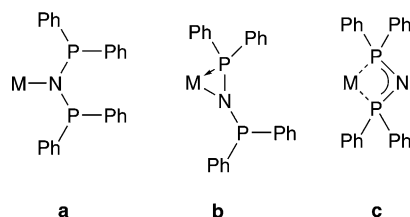
substituent R and the metal. In the reaction of CyN=C=NCy (Cy = cyclohexyl) with [Cp<sub>2</sub>Ti(η<sup>2</sup>-Me<sub>3</sub>SiC<sub>2</sub>SiMe<sub>3</sub>)]<sub>2</sub>, a bimetallic complex was formed, which displayed coordination of the metal fragments to the two nitrogen atoms as well as to the central carbon atom of the substrate (Scheme 1, **D**).<sup>[6]</sup> This coordination type was described before for a bimetallic iron complex.<sup>[7]</sup> By using the zirconocene source [Cp<sub>2</sub>Zr(py)(η<sup>2</sup>-Me<sub>3</sub>SiC<sub>2</sub>SiMe<sub>3</sub>)] in the reaction with carbodiimides, the formation of five-membered heterometallacycloallenes occurred as we have recently described.<sup>[8]</sup>

These results prompted us to investigate reactions with precursors for allylic heterometallacycles, such as *N,N*-bis(diphenylphosphino)amine Ph<sub>2</sub>P-N(H)-PPh<sub>2</sub> (**1**), which to date has only been used as a ligand in its deprotonated form in a few complexes.

[a] M. Haehnel, S. Hansen, Dr. A. Spannenberg, Dr. P. Arndt, Dr. T. Beweries, Prof. Dr. U. Rosenthal  
Leibniz-Institut für Katalyse e. V. an der Universität Rostock  
Albert-Einstein-Strasse 29A, 18059 Rostock (Germany)  
Fax: (+49) 381-1281-51176  
Fax: (+49) 381-1281-51104  
E-mail: uwe.rosenthal@catalysis.de  
torsten.beweries@catalysis.de

Supporting information for this article is available on the WWW under <http://dx.doi.org/10.1002/chem.201201114>.

In general, *N,N*-bis(diphenylphosphino)amide as a ligand can exist in three different binding modes (Scheme 2). *N*-Binding (Scheme 2, **a**) is only known in the complexes  $[(18\text{-crown-6})\text{Cs}\{\text{N}(\text{PPh}_2)_2\}]$  and  $[(\text{PMDTA})\text{K}\{\text{N}(\text{PPh}_2)_2\}]$



Scheme 2. Different coordination modes of the  $\text{Ph}_2\text{P-N-PPh}_2$  moiety at a metal center.

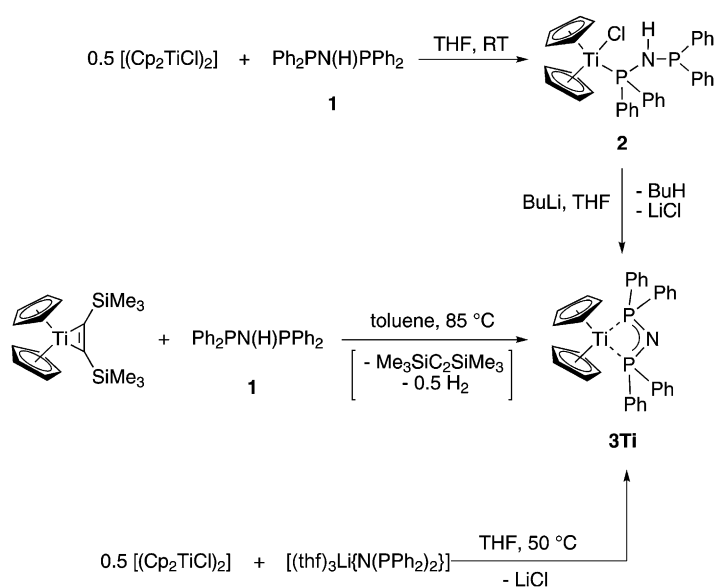
(PMDTA = *N,N,N',N'',N'''*-pentamethyldiethylenetriamine), in which additional interactions of the metal with one or two Ph groups, respectively, were observed.<sup>[9a,b]</sup> *N*-Binding with an additional P-coordination (Scheme 2, **b**) was described for numerous rare earth<sup>[10–13]</sup> and some alkaline earth metal complexes<sup>[12–15]</sup> as well as for the sodium complex  $[(\text{PMDTA})\text{Na}\{\text{N}(\text{PPh}_2)_2\}]$ .<sup>[16]</sup> This coordination mode was also discussed for the lithium complex  $[(\text{thf})_3\text{Li}\{\text{N}(\text{PPh}_2)_2\}]$ .<sup>[9c]</sup> Roesky and co-workers described  $[\text{Cp}_2\text{Zr}(\text{Cl})\{\kappa^2\text{-N,P-N}(\text{PPh}_2)_2\}]$ —the only transition-metal complex with coordination mode **b**.<sup>[17]</sup>

Complexes containing the chelating  $\kappa^2\text{-P,P}(\text{Ph}_2\text{P-N-PPh}_2)$  fragment (Scheme 2, **c**) have been isolated before. However besides the rubidium complex  $[(18\text{-crown-6})\text{Rb}\{\text{N}(\text{PPh}_2)_2\}]$ <sup>[9b]</sup> and the indium complex  $[\text{In}\{\text{N}(\text{PPh}_2)_2\}_3]$ ,<sup>[9c]</sup> only examples with late transition metals, such as iron, nickel, palladium, and platinum, were reported in this context. Ellermann and Wend have prepared  $[\text{CpFe}(\text{CO})(\kappa^2\text{-P,P-Ph}_2\text{P-N-PPh}_2)]$  as the first metallacycle, displaying a cyclic Fe-P-N-P unit at the metal center by salt-metathesis reaction.<sup>[18]</sup> However, the obtained product was only characterized spectroscopically. Kornev and co-workers published a  $\text{Ni}^{\text{II}}$  complex  $[\text{Ni}(\kappa^2\text{-P,P-Ph}_2\text{P-N-PPh}_2)_2]$  containing two PNP moieties coordinated at a single metal center by disproportionation of  $[(\text{Ph}_3\text{P})_2\text{Ni}(\text{SiMe}_3)_2]$  in the presence of  $\text{Ph}_2\text{P-N(H)-PPh}_2$  along with the formation of  $[(\text{Ph}_3\text{P})_2\text{Ni}\{\eta^2\text{-Ph}_2\text{P-N(H)-PPh}_2\}]$ .<sup>[19]</sup> The platinum and iron complexes  $[\{\eta^2\text{-Ph}_2\text{PNP}(\text{Ph}_2)\text{NPPH}_2\}\text{M}(\kappa^2\text{-P,P-Ph}_2\text{P-N-PPh}_2)]$  (M = Fe, Pt) reported by Ellermann et al. were synthesized by the reaction of  $\text{MCl}_2$  and  $[(\text{thf})_3\text{LiN}(\text{PPh}_2)_2]$  in boiling toluene.<sup>[20]</sup> Adding CO to the iron complex resulted in the formation of  $[\{\eta^2\text{-Ph}_2\text{PNP}(\text{Ph}_2)\text{NPPH}_2\}(\text{CO})_2\text{Fe}(\kappa^2\text{-P,P-Ph}_2\text{P-N-PPh}_2)]$ . The first complex of this type, which was characterized by X-ray crystal-structure analysis, was the palladium complex  $[(\text{Et}_3\text{P})(\text{Cl})\text{Pd}(\kappa^2\text{-P,P-Ph}_2\text{P-N-PPh}_2)]$ , obtained by the reaction of  $[\text{PdCl}_2(\text{PET}_3)_2]$  with  $[\text{Li}\{\text{N}(\text{PPh}_2)_2\}]$ .<sup>[21]</sup> In contrast to the lithium complex, in this case, the complexation of the ligand to the metal takes place through a  $\eta^2$ -coordination with the relatively soft, in terms of the HSAB concept, phosphorus atoms.

## Results and Discussion

Reaction of *N,N*-bis(diphenylphosphino)amine (**1**) with  $[(\text{Cp}_2\text{TiCl})_2]$  at elevated temperatures in THF resulted in the formation of the titanocene(III) monochloride complex **2** (Scheme 3). *N,N*-bis(diphenylphosphino)amine acts as a donor ligand to fill up the deficient coordination number of the  $\{\text{Cp}_2\text{TiCl}\}$  fragment. The paramagnetic complex **2** was characterized by mass spectrometry, its molecular-ion peak was found at  $m/z$  599. Green crystals suitable for an X-ray analysis were obtained from a saturated toluene solution at 8 °C.

The molecular structure of complex **2** is shown in Figure 1. The Ti1–P1 bond length was found to be 2.6224(5) Å, which is in the expected range compared with other trivalent titanocene(III) complexes  $[\text{Cp}_2\text{TiCl}(\text{PMe}_2\text{R})]$  (R = Me,<sup>[22]</sup> SiMe<sub>3</sub><sup>[23]</sup>). The structural parameters (N1–H1A...Cl1 unit: N1–H1A 0.80(2), H1A...Cl1 2.62(2),



Scheme 3. Synthesis of the titanocene complexes **2** and **3Ti**.

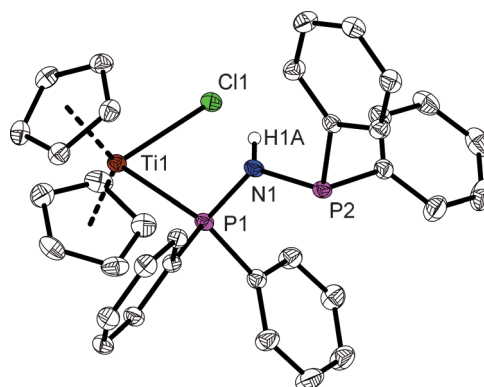
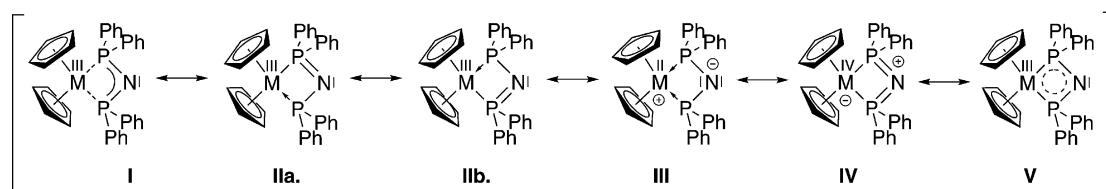


Figure 1. Molecular structure of complex **2**. Hydrogen atoms, except H1A, are omitted for clarity. The thermal ellipsoids correspond to 30% probability.

Scheme 4. Possible resonance forms of complexes **3M**.

$N1\cdots Cl1$  3.283(2) Å;  $N1-H1A\cdots Cl1$  141(2)° indicate a weak hydrogen bond between the chlorine and the hydrogen atom of the amino group.<sup>[24]</sup>

Most interestingly, the titanocene monochloride complex **2** reacted with *n*-butyllithium in THF in a well-predicted way to give complex **3Ti** as the first highly strained four-membered metallacycle of an early transition metal with a *N,N*-bis(diphenylphosphino)amide ligand (Scheme 3). Formation of the dark green  $Ti^{III}$  metallacyclic amide [ $Cp_2Ti(\kappa^2-P,P-Ph_2P-N-PPh_2)$ ] (**3Ti**) occurred selectively and in high yield (85%); oxidation to  $Ti^{IV}$  was not observed. Complex **3Ti** was characterized by mass spectrometry, its molecular ion peak was found at  $m/z$  562.

Additionally, we investigated other ways to obtain the metallacycle **3Ti** (Scheme 3). When we applied the known titanocene source [ $Cp_2Ti(\eta^2-Me_3SiC_2SiMe_3)$ ]<sup>[25]</sup> in combination with the amine **1**, we found that formation of the desired  $Ti^{III}$  complex occurred readily. Moreover, compound **3Ti** can be prepared from the monochloride complex [ $(Cp_2TiCl)_2$ ] and the lithium amide [(*thf*)<sub>3</sub>Li{*N*(*PPh*<sub>2</sub>)<sub>2</sub>}]. It should be noted that in both cases, formation of the metallacycle occurred selectively (yields of 85 and 95%, respectively).

The molecular structure of complex **3Ti** is shown in Figure 2. The titanium center is coordinated by two Cp ligands and the chelating PNP moiety in a strongly distorted

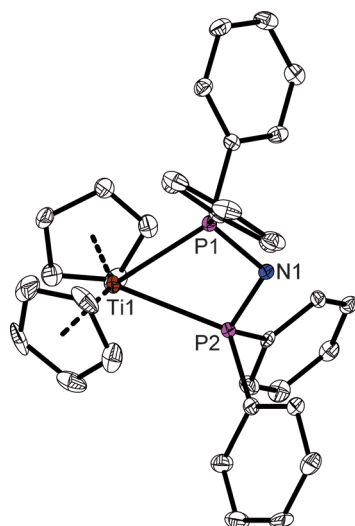
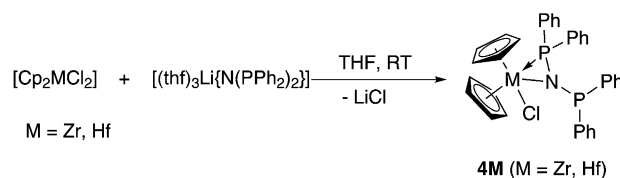


Figure 2. Molecular structure of **3Ti**. Hydrogen atoms, the second molecule of the asymmetric unit, and the solvent molecules (THF) are omitted for clarity. The thermal ellipsoids correspond to 30% probability.

tetrahedral geometry. The  $Ti-P$  distances (2.5997(6)–2.6293(6) Å) are comparable to those in complex **2**. Due to the chelating effect of the ligand, the  $P-N-P$  angle (av 104.7°) is rather small for an  $sp^2$ -hybridised nitrogen atom. The very small  $P-Ti-P$  angle (av 60.1°) proves the high strain of the metallacycle, being even smaller than the  $P-M-P$  angle (64.5–67.4°) in other transition-metal complexes mentioned above.<sup>[20]</sup> This is notable, because the square-planar or octahedral geometry of these complexes and the tetrahedral geometry of the titanium center would suggest the opposite (ideal: square planar/octahedral 90°, tetrahedral 109.5°).

Compared with the  $P-N$  bond lengths in free *N,N*-bis(diphenylphosphino)amine (**1**) (1.692 Å,  $P-N$  single bond),<sup>[26]</sup> the  $P-N$  bond lengths (av. 1.653(3) Å) in the deprotonated ligand bound to a metal are shortened, but longer than a typical  $P=N$  double bond (1.599 Å).<sup>[27]</sup> This indicates a bond order between 1 and 2, which can be attributed to the possible resonance forms for the complex, depicted in Scheme 4.

The reaction of hafnocene dichloride with one equivalent of lithiated *N,N*-bis(diphenylphosphino)amine led, not surprisingly, to the formation of a metallocene(IV) amide complex, which features additional coordination of one of the phosphorus atoms of the ligand (Scheme 5). Complex **4Hf** is

Scheme 5. Synthesis of complexes **4Zr** and **4Hf**.

isostructural to the zirconocene complex [ $Cp_2Zr(Cl)\{\kappa^2-N,P-N(PPh_2)_2\}$ ] (**4Zr**), which was described by Roesky and co-workers<sup>[17]</sup> and characterized by NMR spectroscopy. In complex **4Hf** in solution, two different phosphorus resonances were found at  $\delta=60.3$  and  $-4.7$  ppm with the downfield signal indicating a strong coordination of the phosphorus atom to the hafnium center even in solution. At room temperature, rapid exchange of the coordinating phosphorus atom can be observed by <sup>31</sup>P NMR NOESY spectroscopy, indicating a “flapping” of the *N,N*-bis(diphenylphosphino)amide ligand at the metal center. In <sup>1</sup>H NMR spectra, the resonance of the Cp rings appears as a triplet due to a <sup>3</sup>*J* coupling (<sup>3</sup>*J*<sub>P,H</sub>=8.4 Hz) of the Cp protons with the coordinating phosphorus atom. At  $T=348$  K, both <sup>31</sup>P NMR reso-

nances disappeared, indicating coalescence of the phosphorus atoms at elevated temperatures. Additionally, complex **4Hf** was characterized by mass spectrometry, its  $[M+H]^+$  peak was found at  $m/z$  730.

Colorless crystals of **4Hf** suitable for an X-ray diffraction analysis were obtained from a saturated toluene solution at room temperature. The molecular structure of complex **4Hf** is shown in Figure 3. The hafnium center is coordinated by

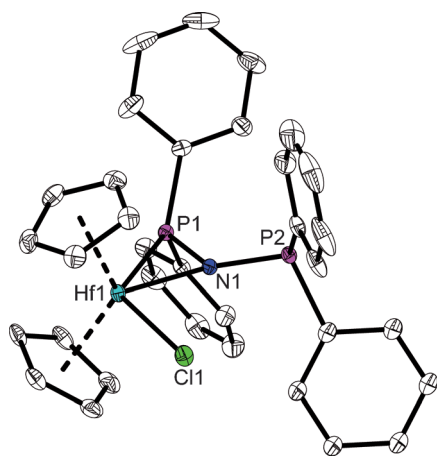


Figure 3. Molecular structure of complex **4Hf**. Hydrogen atoms, the second position of the disordered Ph group, and the solvent molecule (toluene) are omitted for clarity. The thermal ellipsoids correspond to 30% probability.

two Cp units, a chloride ligand, and the *N,N*-bis(diphenylphosphino)amide moiety through N1 and P1 in a  $\eta^2$ -fashion, similar to the Zr complex **4Zr**.<sup>[17]</sup> Hf1, N1, and P1 form a plane with the chloride ligand being 0.26 Å above and the phosphorus atom P2 0.31 Å below this plane. A Hf1–P1 bond length of 2.6248(6) Å was obtained. (cf.  $[\text{Cp}_2\text{Hf}(\text{PMe}_3)(\eta^2\text{-Me}_3\text{SiC}_2\text{SiMe}_3)]$  Hf–P 2.660(1) Å<sup>[28]</sup>).

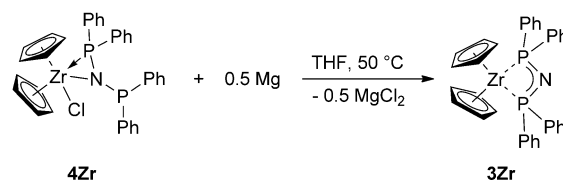
Analysis of the bonding in complex **4Hf** by using DFT methods showed Wiberg bond indices of 0.48 for Hf–P1 and 0.49 for Hf–N as well as 0.94 for N–P1 and 0.80 for N–P2. Compared with the free ligand, the P–N bond orders are significantly decreased (cf. 1.03). Moreover, these values indicate a significant bonding interaction between the metal center and the P and N atoms, respectively. Similar results were found for the isostructural complex **4Zr** (Zr–P1 0.52, Zr–N 0.51, N–P1 0.96, N–P2 0.81; Table 1).

The reaction of complex **4Zr** with magnesium at elevated temperatures in THF resulted in the formation of a very rare Zr<sup>III</sup> complex, the four-membered metallacycle **3Zr** (Scheme 6), which is isostructural to complex **3Ti**. The reaction occurs even with an excess of Mg, impressively corroborating the stability of this Zr<sup>III</sup> complex. This is noteworthy, because normally Zr<sup>III</sup> compounds are very sensitive to possible reduction or disproportionation reactions.<sup>[29]</sup> Additionally, complex **3Zr** was characterized by mass spectrometry, the molecular ion peak was found at  $m/z$  603.

Complex **3Zr** can be obtained as a dark orange compound from concentrated toluene solutions at  $-78^\circ\text{C}$ . The

Table 1. Comparison of selected calculated bond lengths (interatomic distances, respectively) [Å] and angles [°] of complexes **4Ti**, **4Zr**, and **4Hf** with experimental data.

	<b>4Ti</b> (calcd)	<b>4Zr</b> (calcd)	<b>4Zr</b> (exptl) <sup>[17]</sup>	<b>4Hf</b> (calcd)	<b>4Hf</b> (exptl)
P1–M	2.572	2.705	2.649(2)	2.713	2.6248(6)
P2–M	3.776	3.874	3.836	3.826	3.781
P1–N	1.660	1.678	1.642(5)	1.689	1.653(2)
P2–N	1.740	1.748	1.708(5)	1.752	1.708(2)
M–N	2.166	2.269	2.249(5)	2.221	2.208(2)
M–Cl	2.481	2.532	2.518(2)	2.497	2.5085(6)
Ct1–M	2.132	2.290	2.239(3)	2.270	2.224
Ct2–M	2.114	2.273	2.246(3)	2.249	2.211
Ct1–M–Ct2	128.71	127.02	125.94(1)	126.75	127.1
Cl–M–N	81.79	85.09	84.70(14)	86.06	84.50(5)
M–P1–N	56.76	56.70	57.6(2)	54.82	56.83(7)
P1–N–M	83.37	85.11	84.3(2)	86.77	84.36(8)
N–M–P1	39.88	38.19	38.08(1)	38.41	38.81(5)
P1–N–P2	124.26	123.97	124.2(3)	122.69	123.74(12)
M–N–P2	150.18	149.11	151.3(3)	148.48	149.62(11)
Cl–M–N–P2	25.43	24.11	7.94	25.86	26.7(2)
Cl–M–N–P1	–175.06	–174.24	–177.44	–173.60	–174.06(7)



Scheme 6. Synthesis of the metallacycle **3Zr** from complex **4Zr**.

molecular structure of complex **3Zr**, isostructural to complex **3Ti**, is depicted in Figure 4. A comparison of selected bond lengths and angles of **3Ti** and **3Zr** is shown in Table 2. The zirconium center is also coordinated in a strongly distorted tetrahedral geometry. The P–N bond lengths in complex **3Zr** are equivalent and the same as were found in **3Ti**.

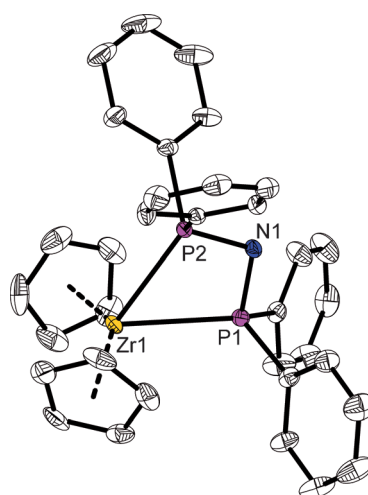


Figure 4. Molecular structure of complex **3Zr**. Hydrogen atoms and the solvent molecules (toluene) are omitted for clarity. The thermal ellipsoids correspond to 30% probability.

Table 2. Comparison of selected calculated and experimental bond lengths (interatomic distances, respectively) [Å] and angles [°] of complexes **3Ti**, **3Zr**, and the computed complex **3Hf**. For complex **3Ti**, all experimental values are averaged.

	<b>3Ti</b> (calcd)	<b>3Ti</b> (exptl)	<b>3Zr</b> (calcd)	<b>3Zr</b> (exptl)	<b>3Hf</b> (calcd)
P1–M	2.637	2.622	2.758	2.7036(6)	2.723
P2–M	2.637	2.604	2.761	2.7130(5)	2.726
P1–N	1.683	1.652	1.685	1.655(2)	1.686
P2–N	1.683	1.654	1.685	1.652(2)	1.686
M...N	3.298	3.270	3.436	3.379	3.410
Ct1–M	2.046	2.034	2.211	2.179	2.173
Ct2–M	2.046	2.043	2.213	2.179	2.176
Ct1–M–Ct2	136.08	136.2	137.24	137.7	136.44
P1–M–P2	60.85	60.1	58.06	57.69(2)	58.53
P1–N–P2	104.98	104.7	105.25	104.43(10)	104.38
N–P1–M	97.09	97.21	98.40	98.81(6)	98.59
N–P2–M	97.09	97.84	98.27	98.54(6)	98.47
NICS <sub>0 Å</sub> [ppm]	–6.06		–4.43		–3.76
NICS <sub>1 Å</sub> [ppm]	–3.39		–4.40		–4.60
Mulliken spin density (at M)	1.40		1.04		0.98

The P–Zr–P angle (57.69(2)°) represents the high strain of the heterometallacycle **3Zr** as shown in **3Ti** and deviates highly from the ideal tetrahedral angle (109.47°).

Attempts to perform a similar reduction reaction starting from the hafnocene complex **4Hf** to get a full set of isostructural heterometallacyclic complexes **3M** failed until now, thus indicating that the reactivity of the hafnocene species is more diverse than for its zirconocene analogue. However, the hypothetical complex **3Hf** was identified as stationary point by DFT analysis and was found to be a minimum from the absence of imaginary harmonic vibrational frequencies (see below), suggesting that this compound should be in principle stable. Further experimental studies to address this issue are under way; the results will be published in due course. In this context, it should be noted that unexpected, yet significant changes in reactivity were observed before when going from zirconocenes to hafnocenes. Examples include C–H and Si–C bond activations in the synthesis of decamethylhafnocene alkyne complexes,<sup>[30]</sup> THF ring-opening reactions<sup>[31]</sup> as well as more recently dinitrogen activation and functionalization at Group 4 metallocenes.<sup>[32]</sup>

**DFT study of the metallacycles 3M:** To get a more detailed picture of the bonding situation in the complexes **3M**, DFT calculations on the BVP86/(6-311+G(d,p)/LANL2DZ) level of theory were performed. The computed structural parameters are in good agreement with those found by X-ray diffraction analysis (Table 2). For comparison, we also determined P–N bond lengths and the P–N–P angle in the free ligand [(Ph<sub>2</sub>P)<sub>2</sub>N]<sup>–</sup> (P–N 1.684 Å, P–N–P 116.91°).

In complex **3Ti**, the Ti<sup>III</sup> center exhibits a Mulliken spin density of 1.40 (cf. Zr 1.04, Hf 0.98). Examination of the charge distribution in the ligand by means of natural-bond orbitals (NBO) analysis revealed that the negative charge is localized at the N atom in all complexes **3M** (for details, see the Supporting Information, Table S1). The bond composi-

Table 3. NBO occupancies, polarizations and Wiberg bond indices (WBI) of the calculated compounds [(Ph<sub>2</sub>P)<sub>2</sub>N]<sup>–</sup>, **3Ti**, **3Zr**, and **3Hf**.

		Occu- pancy [e]	Polarization of Ψ <sub>NBO</sub>	WBI
[(Ph <sub>2</sub> P) <sub>2</sub> N] <sup>–</sup>	N–P	1.975	0.832(sp <sup>2.65</sup> ) + 0.555(sp <sup>4.33</sup> )	1.03
	<sup>α</sup> Ti–P	0.948	0.547(sd <sup>6.67</sup> ) + 0.837(sp <sup>2.23</sup> )	0.60
	<sup>β</sup> Ti–P	0.947	0.522(sd <sup>6.21</sup> ) + 0.853(sp <sup>2.17</sup> )	
<b>3Ti</b>	<sup>α</sup> N–P	0.986	0.834(sp <sup>2.47</sup> ) + 0.552(sp <sup>3.48</sup> )	1.01
	<sup>β</sup> N–P	0.981	0.829(sp <sup>3.00</sup> ) + 0.560(sp <sup>3.55</sup> )	
	<sup>α</sup> Zr–P	0.957	0.484(sd <sup>4.86</sup> ) + 0.875(sp <sup>1.94</sup> )	0.58
<b>3Zr</b>	<sup>β</sup> Zr–P	0.956	0.466(sd <sup>4.83</sup> ) + 0.885(sp <sup>1.90</sup> )	
	<sup>α</sup> N–P	0.986	0.833(sp <sup>2.44</sup> ) + 0.554(sp <sup>3.67</sup> )	1.01
	<sup>β</sup> N–P	0.981	0.826(sp <sup>3.02</sup> ) + 0.563(sp <sup>3.73</sup> )	
<b>3Hf</b>	<sup>α</sup> Hf–P	0.959	0.471(sd <sup>3.32</sup> ) + 0.882(sp <sup>1.77</sup> )	0.58
	<sup>β</sup> Hf–P	0.959	0.455(sd <sup>3.71</sup> ) + 0.890(sp <sup>1.74</sup> )	
	<sup>α</sup> N–P	0.985	0.834(sp <sup>2.39</sup> ) + 0.552(sp <sup>3.73</sup> )	1.00
	<sup>β</sup> N–P	0.980	0.826(sp <sup>3.05</sup> ) + 0.563(sp <sup>3.83</sup> )	

tions on the basis of NBO are summarized in Table 3. The NICS<sub>0 Å</sub><sup>[33]</sup> values of –6.06 ppm for Ti, –4.43 ppm for Zr, and –3.76 ppm for Hf indicate in-plane aromaticity in the heterometallacycle, similarly as we observed before in a theoretical study of Group 4 metallocene sulfurdiimide complexes<sup>[5]</sup> and Group 4 metallocene bis(trimethylsilyl)acetylene complexes.<sup>[34]</sup> The NBO analysis suggests that there are two highly polarized Ti–P σ bonds with occupancies of approximately 95% and two P–N σ bonds, each having a high occupancy of 98%. This, along with the Wiberg bond indices (Table 3), reveals the presence of a four-membered σ skeleton for complex **3Ti**. An interannular bonding contribution between the metal center and the central N can be excluded by comparing the contact distances and the sum of the covalence radii (*r*<sub>cov</sub>; calculated contacts: Ti...N 3.30 Å, Zr...N 3.44 Å and Hf...N 3.41 Å, respectively; Σ*r*<sub>cov</sub>: Ti–N 2.07 Å, Zr–N 2.25 Å, and Hf–N 2.23 Å, respectively<sup>[35]</sup>). It should be noted that the small differences between Ti on one side and Zr and Hf on the other side are in good agreement with other theoretical studies of Group 4 metallocenes (Table 3).<sup>[34]</sup>

## Conclusion

In summary, we presented a detailed experimental and theoretical study on the coordination chemistry of the known *N,N*-bis(diphenylphosphino)amide ligand to Group 4 metallocene fragments {Cp<sub>2</sub>M} (M = Ti, Zr, Hf). Depending on the metal, its oxidation state, and the nature of the ligand precursor (i.e., free amine vs. its Li salt), different products are obtained, including M<sup>III</sup> and M<sup>IV</sup> chlorides as well as the metallacycles **3M** (M = Ti, Zr). For M = Ti, the latter species can be generated in several ways, namely reduction of the amine with [Cp<sub>2</sub>Ti], salt metathesis from [(Cp<sub>2</sub>TiCl)<sub>2</sub>] and the Li salt or by reaction of the titanocene monochloride **2**. Complex **3Zr** was readily obtained by reduction of the Zr<sup>IV</sup> chloro complex **4Zr**. DFT analysis of the metallacycles **3M** revealed that the stability of these species can be attributed to a strong cyclic delocalization of electrons in the ring, sim-

ilarly as observed before for titanocene and zirconocene sulfurdiimide complexes.

## Experimental Section

**General:** All manipulations were carried out in an oxygen- and moisture-free argon atmosphere by using standard Schlenk and glovebox techniques. All solvents were dried over sodium/benzophenone and freshly distilled from sodium tetraethylaluminate prior to use. *N,N*-bis(diphenylphosphino)amine was purchased from ABCR chemicals and used as received.  $[\text{Cp}_2\text{TiCl}_2]$  and  $[\text{Cp}_2\text{ZrCl}_2]$  were purchased from Sigma-Aldrich and used as received.  $[(\text{Cp}_2\text{TiCl})_2]$  and  $[\text{Cp}_2\text{HfCl}_2]$  were purchased from MCAT (Metallocene Catalysts & Life Science Technologies, Konstanz, Germany) and used without further purification.  $[\text{Cp}_2\text{Ti}(\eta^2\text{-Me}_3\text{SiC}_2\text{SiMe}_3)]^{25]}$  and  $[(\text{thf})_2\text{Li}[\text{N}(\text{PPh}_2)_2]]^{9]}$  were prepared according to described procedures. For NMR analysis, Bruker AV300 spectrometer was used.  $^1\text{H}$  and  $^{13}\text{C}$  NMR chemical shifts are given in ppm ( $\delta$ ) and were referenced by using the chemical shifts of residual protio solvent resonances:  $[\text{D}_6]$ benzene ( $\delta_{\text{H}}=7.16$ ,  $\delta_{\text{C}}=128.0$  ppm). For elemental analysis, Leco CHNS-932 elemental-analyzer machine was used. For melting points determination, Büchi 535 apparatus was used. Melting points are uncorrected and were measured in sealed capillaries.

**Preparation of complex 2 from  $[(\text{Cp}_2\text{TiCl})_2]$ :** To a stirred solution of  $[(\text{Cp}_2\text{TiCl})_2]$  (269 mg, 0.63 mmol) in THF (10 mL), a solution of *N,N*-bis(diphenylphosphino)amine (**1**; 520 mg, 1.35 mmol) in THF (15 mL) was added. While the reaction mixture was stirred at 50 °C for 16 h, its color turned to dark green. After cooling to RT, the solvent was removed in vacuum. The dark green residue was dried in vacuum. Yield: 720 mg (95 %); m.p. 139 °C (decomp under Ar); MS (CI, *iso*-butane):  $m/z$  (%): 599  $[M]^+$ , 563  $[M-\text{Cl}]^+$ ; elemental analysis calcd (%) for  $\text{C}_{34}\text{H}_{31}\text{ClNP}_2\text{Ti}$  (598.88 g mol<sup>-1</sup>): C 68.19, H 5.22, N 2.34; found: C 68.22, H 5.31, N 2.49; Crystals suitable for X-ray diffraction analysis were grown from a saturated toluene solution at 8 °C.

**Preparation of complex 3Ti from  $[\text{Cp}_2\text{Ti}(\eta^2\text{-Me}_3\text{SiC}_2\text{SiMe}_3)]$ :** To a stirred solution of  $[\text{Cp}_2\text{Ti}(\eta^2\text{-Me}_3\text{SiC}_2\text{SiMe}_3)]$  (542 mg, 1.56 mmol) in toluene (10 mL), a solution of *N,N*-bis(diphenylphosphino)amine (**1**; 628 mg, 1.63 mmol) in toluene (10 mL) was added. After stirring the reaction mixture for three days at 85 °C, the color turned from light brown to dark brown. The mixture was cooled to RT, and all volatiles were removed in vacuum. The dark brown residue was dissolved in mixture of THF/*n*-hexane (3:1; 20 mL) and stored at -30 °C for three days to give dark green crystals, which were filtered, washed with cold *n*-hexane (3 mL), and dried in vacuum. Yield: 746 mg (85 %); m.p. 111 °C (decomp under Ar); MS (EI, 70 eV):  $m/z$  (%): 562  $[M]^+$ , 385  $[M-\text{Cp}_2\text{Ti}]^+$ , 377  $[M-\text{PPh}_2]^+$ , 178  $[\text{Cp}_2\text{Ti}]^+$ ; elemental analysis calcd (%) for  $\text{C}_{34}\text{H}_{30}\text{NP}_2\text{Ti}\cdot\text{THF}$  (562.42 g mol<sup>-1</sup>): C 71.93; H 6.04, N 2.21; found: C 72.03, H 6.04, N 2.27. Crystals suitable for X-ray diffraction analysis were obtained from a saturated solution of THF at 8 °C.

**Preparation of complex 3Ti from  $[(\text{Cp}_2\text{TiCl})_2]$ :** To a stirred solution of  $[(\text{Cp}_2\text{TiCl})_2]$  (245 mg, 0.574 mmol) in THF (10 mL), a solution of  $[(\text{thf})_2\text{Li}[\text{N}(\text{PPh}_2)_2]]$  (442 mg, 1.15 mmol) in THF (10 mL) was added. The reaction mixture was stirred at 50 °C for 8 h. After cooling to RT, the solvent was removed in vacuum. The dark green residue was suspended in toluene (20 mL) and filtered. All volatiles were removed in vacuum, and the green precipitate was dried in vacuum. Yield: 716 mg (95 %).

**Preparation of 3Ti from 2:** To a stirred solution of **2** (152 mg, 0.254 mmol) in THF (10 mL), a solution of *n*-butyllithium in hexane (1.6 M, 0.24 mL, 0.38 mmol) was added. The light green solution turned dark green immediately. The solvent was removed in vacuum, and the dark green residue was suspended in toluene (20 mL of) and filtered. All volatiles were removed in vacuum, and the dark green precipitate was dried in vacuum. Yield: 122 mg (85 %).

**Alternative synthesis of 4Zr:**<sup>17]</sup> To a stirred solution of *N,N*-bis(diphenylphosphino)amine (380 mg, 0.99 mmol) in THF (20 mL), a solution of *n*-butyllithium in *n*-hexane (1.6 M, 0.74 mL, 1.18 mmol) was added at RT. After stirring the reaction mixture for one hour, the color turned to light

yellow. The mixture was dropped slowly into a solution of  $[\text{Cp}_2\text{ZrCl}_2]$  (288 mg, 0.99 mmol) in THF (15 mL). After stirring for three days, all volatiles were removed in vacuum, and the yellow residue was suspended in toluene (40 mL), filtered, and dried in vacuum to give a pale yellow product. Yield: 504 mg (80 %).  $^1\text{H}$  NMR ( $[\text{D}_6]$ benzene, 300 MHz, 296 K):  $\delta=7.93$  (p,  $^3J=8.1$  Hz, 8H, Ph), 7.22 (t,  $^3J=6.9$  Hz, 4H, Ph), 7.00 (m, 8H, Ph), 5.81 ppm (s, 10H, Cp).  $^{31}\text{P}$  NMR ( $[\text{D}_6]$ benzene, 300 MHz, 296 K):  $\delta=61.24$ , -4.49 ppm.

**Preparation of 4Hf:** To a stirred solution of *N,N*-bis(diphenylphosphino)amine (410 mg, 1.06 mmol) in THF (20 mL), a solution of *n*-butyllithium in hexane (2.5 M, 0.47 mL, 1.17 mmol) was added at RT. After stirring the reaction mixture for 2 h, the color turned to light yellow. The mixture was dropped slowly into a solution of  $[\text{Cp}_2\text{HfCl}_2]$  (404 mg, 1.06 mmol) in THF (15 mL). After stirring for three days, all volatiles were removed in vacuum, and the yellow residue was suspended in toluene (40 mL), filtered, and concentrated to a volume of 4 mL in vacuum. The precipitated product was dissolved at 80 °C. Slow cooling to RT gave colorless crystals suitable for X-ray diffraction analysis; crystals were filtered, washed with cold toluene, and dried in vacuum. The mother liquor was cooled to -78 °C to complete crystallization. Overall yield: 695 mg (90 %); m.p. 153 °C (decomp under Ar);  $^1\text{H}$  NMR ( $[\text{D}_6]$ benzene, 300 MHz, 296 K):  $\delta=7.92$  (t,  $^3J=7.5$  Hz, 8H, Ph), 7.07 (m, 12H, Ph), 5.78 ppm (t,  $^3J=8.4$  Hz, 10H, Cp).  $^{13}\text{C}$  NMR ( $[\text{D}_6]$ benzene, 300 MHz, 296 K):  $\delta=133.16$ -128.79 (Ph), 110.62 ppm (s, Cp);  $^{31}\text{P}\{^1\text{H}\}$  NMR ( $[\text{D}_6]$ benzene, 300 MHz, 296 K):  $\delta=60.26$ , -4.72 ppm; elemental analysis calcd (%) for  $\text{C}_{34}\text{H}_{30}\text{ClHfNP}_2$  (728.50 g mol<sup>-1</sup>): C 56.06, H 4.12, N 1.92; found: C 56.08, H 4.15, N 2.06; MS (CI, *iso*-butane):  $m/z$  (%): 730  $[M+\text{H}]^+$ .

**Preparation of 3Zr from 4Zr:** Complex **4Zr** (126 mg, 0.197 mmol) and magnesium (5 mg, 0.206 mmol) were suspended in THF (10 mL) and heated to 50 °C for 3.5 h. The color slowly changed from pale yellow to orange and later to dark brown. After cooling to RT, all volatiles were removed in vacuum, and the dark brown precipitate was suspended in toluene (20 mL) and filtered. The solution was concentrated to 10 mL and stored at -78 °C to give dark orange crystals of **3Zr** suitable for X-ray analysis; crystals were filtered, washed with cold toluene, and dried in vacuum. Yield: 65 mg (55 %); m.p. 146 °C (decomp under Ar); elemental analysis calcd (%) for  $\text{C}_{34}\text{H}_{30}\text{NP}_2\text{Zr}$  (605.78 g mol<sup>-1</sup>): C 67.41, H 4.99, N 2.31; found: C 66.18, H 5.28, N 2.17; MS (EI, 70 eV):  $m/z$  (%): 604  $[M]^+$ , 385  $[M-\text{Cp}_2\text{Ti}]^+$ , 262  $[M-\text{NPPh}_2]^+$ .

**Computational details:** DFT calculations on basis of the BVP86<sup>36]</sup> level of theory were performed applying the ECP basis set LANL2DZ<sup>37]</sup> on the Group 4 metals and 6-311+G(d,p) to the other elements, respectively, followed by NBO 5.9<sup>38]</sup> analyses. All calculations have been carried out with the Gaussian 09, Rev. A0.2<sup>39]</sup> suite of programs.

**Crystallographic details:** Data were collected using graphite-monochromated  $\text{MoK}\alpha$  radiation ( $\lambda=0.71073$  Å) on the following diffractometers: STOE IPDS II (complex **2**) and Bruker Kappa APEX II Duo (complexes **3Ti**, **4Hf**, and **3Zr**), respectively. The structures were solved by direct methods (SHELXS-97) and refined by full-matrix least-squares procedures on  $F^2$  (SHELXL-97).<sup>40]</sup> CCDC-873829 (**2**), CCDC-873826 (**3Ti**), CCDC-873827 (**4Hf**), and CCDC-873828 (**3Zr**) contain the supplementary crystallographic data for this paper. These data can be obtained free of charge from The Cambridge Crystallographic Data Centre via [www.ccdc.cam.ac.uk/data\\_request/cif](http://www.ccdc.cam.ac.uk/data_request/cif).

**Crystal data for 2:**  $\text{C}_{34}\text{H}_{31}\text{ClNP}_2\text{Ti}$ ;  $M=598.89$  g mol<sup>-1</sup>; triclinic; space group  $P\bar{1}$ ;  $a=9.3644(4)$ ,  $b=9.7193(4)$ ,  $c=17.3054(8)$  Å;  $\alpha=84.095(4)$ ,  $\beta=80.708(3)$ ,  $\gamma=70.022(3)^\circ$ ;  $V=1458.9(1)$  Å<sup>3</sup>;  $T=150(2)$  K;  $Z=2$ ,  $\rho_{\text{calcd}}=1.363$  g cm<sup>-3</sup>;  $\mu=0.519$  mm<sup>-1</sup>; absorption correction: numerical (max. and min. transmission: 0.96 and 0.86); 27795 reflections measured; 7855 independent reflections ( $R_{\text{int}}=0.0376$ ); final  $R$  values [ $I>2\sigma(I)$ ]:  $R_1=0.0316$ ;  $wR_2=0.0669$ ; final  $R$  values (all data):  $R_1=0.0529$ ;  $wR_2=0.0701$ ; GOF on  $F^2=0.856$ , 356 parameters.

**Crystal data for 3Ti:**  $\text{C}_{34}\text{H}_{30}\text{NP}_2\text{Ti}\cdot\text{THF}$ ;  $M=634.53$  g mol<sup>-1</sup>; monoclinic; space group  $Cc$ ;  $a=26.7399(5)$ ,  $b=16.9826(3)$ ,  $c=17.4040(6)$  Å;  $\beta=126.169(1)^\circ$ ;  $V=6380.2(3)$  Å<sup>3</sup>;  $T=150(2)$  K;  $Z=8$ ;  $\rho_{\text{calcd}}=1.321$  g cm<sup>-3</sup>;  $\mu=0.400$  mm<sup>-1</sup>; absorption correction: multiscan (max. and min. transmission: 0.75 and 0.67); 56620 reflections measured; 14374 independent reflections ( $R_{\text{int}}=0.0372$ ); final  $R$  values [ $I>2\sigma(I)$ ]:  $R_1=0.0338$ ;  $wR_2=$

0.0796; final  $R$  values (all data):  $R_1=0.0405$ ;  $wR_2=0.0830$ ; GOF on  $F^2=1.018$ , 720 parameters.

**Crystal data for 4Hf:**  $C_{34}H_{30}ClHfNP_2$ -toluene;  $M=820.60$  g mol $^{-1}$ ; triclinic; space group  $P\bar{1}$ ;  $a=10.2413(2)$ ,  $b=11.6123(2)$ ,  $c=14.9773(3)$  Å;  $\alpha=83.569(1)$ ,  $\beta=87.645(1)$ ,  $\gamma=88.005(1)^\circ$ ;  $V=1767.65(6)$  Å $^3$ ;  $T=150(2)$  K;  $Z=2$ ;  $\rho_{\text{calc}}=1.542$  g cm $^{-3}$ ;  $\mu=3.147$  mm $^{-1}$ ; absorption correction: multi-scan (max. and min. transmission: 0.75 and 0.56); 59425 reflections measured; 8122 independent reflections ( $R_{\text{int}}=0.029$ ); final  $R$  values [ $I>2\sigma(I)$ ]:  $R_1=0.0215$ ;  $wR_2=0.0546$ ; final  $R$  values (all data):  $R_1=0.0235$ ;  $wR_2=0.0563$ ; GOF on  $F^2=1.056$ , 389 parameters.

**Crystal data for 3Zr:**  $C_{34}H_{30}NP_2Zr$ -1.6 toluene;  $M=753.16$  g mol $^{-1}$ ; monoclinic; space group  $P2_1/n$ ;  $a=9.0330(2)$ ,  $b=23.6868(5)$ ,  $c=18.3998(4)$  Å;  $\beta=100.376(1)^\circ$ ;  $V=3872.49(15)$  Å $^3$ ;  $T=150(2)$  K;  $Z=4$ ;  $\rho_{\text{calc}}=1.292$  g cm $^{-3}$ ;  $\mu=0.398$  mm $^{-1}$ ; absorption correction: numerical (max. and min. transmission: 1.00 and 0.87); 83206 reflections measured; 9592 independent reflections ( $R_{\text{int}}=0.0408$ ); final  $R$  values [ $I>2\sigma(I)$ ]:  $R_1=0.0386$ ;  $wR_2=0.1005$ ; final  $R$  values (all data):  $R_1=0.0508$ ;  $wR_2=0.1080$ ; GOF on  $F^2=1.060$ , 391 parameters.

## Acknowledgements

We would like to thank our technical and analytical staff for assistance as well as Dr. H. Jiao and Dr. W. Baumann for fruitful discussions. Financial support by the Deutsche Forschungsgemeinschaft (RO 1269/7-2 and RO 1269/8-1) is gratefully acknowledged.

- U. Rosenthal, V. V. Burlakov, M. A. Bach, T. Beweries, *Chem. Soc. Rev.* **2007**, 36, 719–728.
- U. Rosenthal, V. V. Burlakov, P. Arndt, W. Baumann, A. Spannenberg, *Organometallics* **2003**, 22, 884–900.
- a) A. Ohff, S. Pulst, C. Lefeber, N. Peulecke, P. Arndt, V. V. Burlakov, U. Rosenthal, *Synlett* **1996**, 111–118; b) U. Rosenthal, V. V. Burlakov in *Titanium and Zirconium in Organic Synthesis* (Ed.: I. Marek), Wiley-VCH, Weinheim, **2003**, pp. 355–386.
- S. Roy, E. D. Jemmis, A. Schulz, T. Beweries, U. Rosenthal, *Angew. Chem.* **2012**, 124, 5442–5446; *Angew. Chem. Int. Ed.* **2012**, 51, 5347–5350.
- K. Kaleta, M. Ruhmann, O. Theilmann, S. Roy, T. Beweries, P. Arndt, A. Villinger, E. D. Jemmis, A. Schulz, U. Rosenthal, *Eur. J. Inorg. Chem.* **2012**, 611–617.
- O. Theilmann, M. Ruhmann, A. Villinger, A. Schulz, W. W. Seidel, K. Kaleta, T. Beweries, P. Arndt, U. Rosenthal, *Angew. Chem.* **2010**, 122, 9469–9473; *Angew. Chem. Int. Ed.* **2010**, 49, 9282–9285.
- J. Doherty, A. R. Manning, F. S. Stephens, *Inorg. Chem.* **1982**, 21, 3332–3335.
- K. Kaleta, M. Ruhmann, O. Theilmann, T. Beweries, S. Roy, P. Arndt, A. Villinger, E. D. Jemmis, A. Schulz, U. Rosenthal, *J. Am. Chem. Soc.* **2011**, 133, 5463–5473.
- a) J. Ellermann, W. Bauer, M. Schutz, F. W. Heinemann, M. Moll, *Monatsh. Chem.* **1998**, 129, 547–566; b) J. Ellermann, M. Schütz, F. W. Heinemann, M. Moll, W. Bauer, *Chem. Ber.* **1997**, 130, 141–144; c) T. Kremer, F. Hampel, F. A. Knoch, W. Bauer, A. Schmidt, P. Gabold, M. Schutz, J. Ellermann, P. v. R. Schleyer, *Organometallics* **1996**, 15, 4776–4782; Niecke and co-workers also published [(thf) $_3$ Li{N(PPh $_2$ ) $_2$ }], see: M. Nieger, N. Poetschke, E. Niecke, K. Airola, *Z. Kristallogr. New Cryst. Struct.* **1997**, 212, 247–248; A. Winkler, F. W. Heinemann, V. Carcia-Montalvo, M. Moll, J. Ellermann, *Eur. J. Inorg. Chem.* **1998**, 437–444.
- M. T. Gamer, P. W. Roesky, *Inorg. Chem.* **2004**, 43, 4903–4906.
- M. T. Gamer, G. Canseco-Melchor, P. W. Roesky, *Z. Anorg. Allg. Chem.* **2003**, 629, 2113–2116.
- P. W. Roesky, *Inorg. Chem.* **2005**, 44, 798–802.
- T. K. Panda, M. T. Gamer, P. W. Roesky, *Inorg. Chim. Acta* **2006**, 359, 4765–4768.
- R. A. Kemp, D. A. Dickie, A. M. Felix, Private Communication to the Cambridge Structural Database, **2007** (CCDC-661036).
- S. Datta, M. T. Gamer, P. W. Roesky, *Dalton Trans.* **2008**, 2839–2843.
- J. Ellermann, M. Schütz, F. W. Heinemann, M. Moll, *Z. Anorg. Allg. Chem.* **1998**, 624, 257–262.
- M. T. Gamer, M. Rastätter, P. W. Roesky, *Z. Anorg. Allg. Chem.* **2002**, 628, 2269–2272.
- J. Ellermann, W. Wend, *Z. Anorg. Allg. Chem.* **1986**, 543, 169–185.
- V. V. Sushev, A. N. Kornev, Y. V. Fedotova, Y. A. Kursky, T. G. Mushtina, G. A. Abakumov, L. N. Zakharov, A. L. Rheingold, *J. Organomet. Chem.* **2003**, 676, 89–93.
- J. Ellermann, P. Gabold, C. Schelle, F. A. Knoch, M. Moll, W. Bauer, *Z. Anorg. Allg. Chem.* **1995**, 621, 1832–1843.
- M. Gómez, G. Muller, J. Sales, X. Solans, *J. Chem. Soc. Dalton Trans.* **1993**, 221–225.
- L. B. Kool, M. D. Rausch, H. G. Alt, M. Herberhold, B. Wolf, U. Thewalt, *J. Organomet. Chem.* **1985**, 297, 159–169.
- R. Payne, J. Hachgenei, G. Fritz, D. Fenske, *Z. Naturforsch. B* **1986**, 41, 1535–1540.
- G. R. Desiraju, T. Steiner, *The Weak Hydrogen Bond: In Structural Chemistry and Biology*, Oxford University Press, Oxford, **1999**.
- V. V. Burlakov, U. Rosenthal, P. V. Petrovskii, V. B. Shur, M. E. Vol'pin, *Organomet. Chem. USSR* **1988**, 1, 526–528.
- a) H. Nöth, E. Z. Fluck, *Z. Naturforsch. B* **1984**, 39, 744; b) A. L. Rheingold, Private Communication to the Cambridge Structural Database (CCDC-268932).
- F. H. Allen, O. Kennard, D. G. Watson, *J. Chem. Soc., Perkin Trans.* **1987**, 2, S1–S19.
- T. Beweries, V. V. Burlakov, M. A. Bach, P. Arndt, W. Baumann, A. Spannenberg, U. Rosenthal, *Organometallics* **2007**, 26, 247–249.
- P. C. Wailes, H. Weigold, *J. Organomet. Chem.* **1971**, 28, 91–95.
- T. Beweries, V. V. Burlakov, M. A. Bach, S. Peitz, P. Arndt, W. Baumann, A. Spannenberg, U. Rosenthal, B. Pathak, E. D. Jemmis, *Angew. Chem.* **2007**, 119, 7031–7035; *Angew. Chem. Int. Ed.* **2007**, 46, 6907–6910.
- T. Beweries, U. Jäger-Fiedler, M. A. Bach, V. V. Burlakov, P. Arndt, W. Baumann, A. Spannenberg, U. Rosenthal, *Organometallics* **2007**, 26, 3000–3004.
- a) D. J. Knobloch, E. Lobkovsky, P. J. Chirik, *J. Am. Chem. Soc.* **2010**, 132, 10553–10564; b) D. J. Knobloch, E. Lobkovsky, P. J. Chirik, *Nat. Chem.* **2010**, 2, 30–35.
- a) P. von R. Schleyer, C. Maerker, A. Dransfeld, H. Jiao, N. J. R. van E. Hommes, *J. Am. Chem. Soc.* **1996**, 118, 6317–6318; b) P. von R. Schleyer, H. Jiao, N. J. R. van E. Hommes, G. V. Malkin, O. L. Malkina, *J. Am. Chem. Soc.* **1997**, 119, 12669–12670; c) P. von R. Schleyer, M. Manoharan, Z.-X. Wang, B. Kiran, H. Jiao, R. Puchta, N. J. R. van E. Hommes, *Org. Lett.* **2001**, 3, 2465–2468.
- E. D. Jemmis, S. Roy, V. V. Burlakov, H. Jiao, M. Klahn, S. Hansen, U. Rosenthal, *Organometallics* **2010**, 29, 76–81.
- P. Pyykkö, M. Atsumi, *Chem. Eur. J.* **2009**, 15, 12770–12779.
- a) A. D. Becke, *Phys. Rev. A* **1988**, 38, 3098–3100; b) S. H. Vosko, L. Wilk, M. Nusair, *Can. J. Phys.* **1980**, 58, 1200–1211; c) J. P. Perdew, *Phys. Rev. B* **1986**, 33, 8822–8824.
- a) P. J. Hay, W. R. Wadt, *J. Chem. Phys.* **1985**, 82, 270–283; b) W. R. Wadt, P. J. Hay, *J. Chem. Phys.* **1985**, 82, 284–298; c) P. J. Hay, W. R. Wadt, *J. Chem. Phys.* **1985**, 82, 299–310.
- NBO 5.9, E. D. Glendening, J. K. Badenhoop, A. E. Reed, J. E. Carpenter, J. A. Bohmann, C. M. Morales, F. Weinhold (Theoretical Chemistry Institute, University of Wisconsin, Madison, **2009**); <http://www.chem.wisc.edu/~nbo5>.
- Gaussian 09, Revision A02, M. J. Frisch, G. W. Trucks, H. B. Schlegel, G. E. Scuseria, M. A. Robb, J. R. Cheeseman, G. Scalmani, V. Barone, B. Mennucci, G. A. Petersson, H. Nakatsuji, M. Caricato, X. Li, H. P. Hratchian, A. F. Izmaylov, J. Bloino, G. Zheng, J. L. Sonnenberg, M. Hada, M. Ehara, K. Toyota, R. Fukuda, J. Hasegawa, M. Ishida, T. Nakajima, Y. Honda, O. Kitao, H. Nakai, T. Vreven, J. A. Montgomery, Jr., J. E. Peralta, F. Ogliaro, M. Bearpark, J. J. Heyd, E. Brothers, K. N. Kudin, V. N. Staroverov, R. Kobayashi, J.

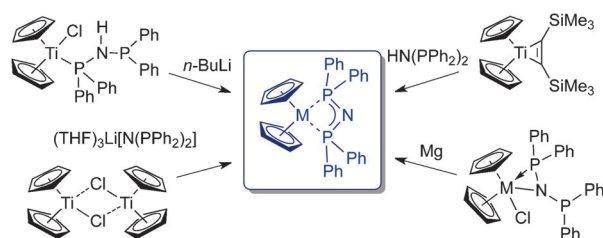
Normand, K. Raghavachari, A. Rendell, J. C. Burant, S. S. Iyengar, J. Tomasi, M. Cossi, N. Rega, J. M. Millam, M. Klene, J. E. Knox, J. B. Cross, V. Bakken, C. Adamo, J. Jaramillo, R. Gomperts, R. E. Stratmann, O. Yazyev, A. J. Austin, R. Cammi, C. Pomelli, J. W. Ochterski, R. L. Martin, K. Morokuma, V. G. Zakrzewski, G. A. Voth, P. Salvador, J. J. Dannenberg, S. Dapprich, A. D. Daniels, Ö.

Farkas, J. B. Foresman, J. V. Ortiz, J. Cioslowski, D. J. Fox, Gaussian, Inc., Wallingford CT, 2009.

[40] G. M. Sheldrick, *Acta Crystallogr. Sect. A* **2008**, *64*, 112–122.

Received: April 2, 2012

Published online: ■ ■ ■, 0000



**All roads lead to Rome:** Heterometallacyclic complexes of the type  $[\text{Cp}_2\text{M}(\kappa^2\text{-P,P-Ph}_2\text{P-N-PPh}_2)]$  ( $\text{Cp} = \eta^5\text{-cyclopentadienyl}$ ;  $\text{M} = \text{Ti, Zr}$ ) can be prepared by using four different synthetic pathways (see scheme). All

routes yielded the corresponding metallacycles in very high yields. Analysis of the structure and bonding of these complexes revealed that in-plane aromaticity plays an important role for the stabilization of these species.

## Metallacycles

M. Haehnel, S. Hansen,  
A. Spannenberg, P. Arndt,  
T. Beweries,\* U. Rosenthal\*



## Highly Strained Heterometallacycles of Group 4 Metallocenes with Bis(diphenylphosphino)amide Ligands



### All roads lead to Rome...

...and to the heterometallacycle  $[\text{Cp}_2\text{M}(\kappa^2\text{-P,P-Ph}_2\text{P-N-PPh}_2)]$ . In their Communication on page ■ ff., U. Rosenthal, T. Beweries et al. describe four different, yet straightforward ways of synthesising unusual four-membered metallacycles of Group 4 metallocenes based on a bis-(diphenyl)amide ligand framework. The cover picture shows the drawing of the Colosseum as a metaphor for the metallacyclic product complex and roman roads symbolising the synthetic pathways leading to it.

